Stability of $^{100}_{50}$Sn$_{50}$ Deduced from Excited States in $^{99}_{48}$Cd$_{51}$

M. Lipoglavšek,[1,2] J. Cederkäll,[3] M. Palacz,[3,4] J. Persson,[1] A. Ataç,[1] J. Blomqvist,[3] C. Fahlander,[1] H. Grawe,[5] A. Johnson,[3] A. Kerek,[3] W. Klamra,[3] J. Kownacki,[6] A. Likar,[2] L.-O. Norlin,[3] J. Nyberg,[1] R. Schubart,[7] D. Seweryniak,[1,8] G. de Angelis,[9] P. Bednarczyk,[9] Zs. Dombrádi,[10] D. Foltescu,[11] D. Jerrestam,[12] S. Juutinen,[13] E. Mäkelä,[13] G. Perez,[10] M. de Poli,[9] H. A. Roth,[11] T. Shizuma,[14] Ö. Skeppstedt,[11] G. Sletten,[14] S. Törmänen,[13] and T. Vass[10]

[1]*The Svedberg Laboratory and Department of Radiation Sciences, Uppsala University, Box 533, S-75121 Uppsala, Sweden*
[2]*J. Stefan Institute, Ljubljana, Slovenia*
[3]*Department of Physics, Royal Institute of Technology, Stockholm, Sweden*
[4]*Soltan Institute for Nuclear Studies, Świerk, Poland*
[5]*Hahn-Meitner Institute, Berlin, Germany*
[6]*Heavy Ion Laboratory, University of Warsaw, Warsaw, Poland*
[7]*II. Physikalisches Institut, Universität Göttingen, Göttingen, Germany*
[8]*Institute of Experimental Physics, University of Warsaw, Warsaw, Poland*
[9]*INFN, Laboratori Nazionali di Legnaro, Legnaro (Padova), Italy*
[10]*Institute of Nuclear Research, Hungarian Academy of Sciences, Debrecen, Hungary*
[11]*Chalmers University of Technology, Gothenburg, Sweden*
[12]*Department of Neutron Research, Uppsala University, Nyköping, Sweden*
[13]*Department of Physics, University of Jyväskylä, Jyväskylä, Finland*
[14]*Niels Bohr Institute, University of Copenhagen, Copenhagen, Denmark*
(Received 14 September 1995)

Excited states of neutron deficient nuclei close to ^{100}Sn were investigated in an in-beam spectroscopic experiment using the NORDBALL detector array. Excited states in ^{99}Cd were identified for the first time. The measured half-life of an isomeric state in ^{99}Cd indicates that the stability with respect to quadrupole shape changes is as large in ^{100}Sn as for other heavy doubly magic nuclei.

PACS numbers: 23.20.Lv, 21.10.Tg, 25.70.Gh, 27.60.+j

The region of nuclei near ^{100}Sn has recently come in focus for studies of nuclear structure. The reason is that ^{100}Sn is the heaviest $N = Z$ nucleus, which may show strong shell closure and is accessible to experimental investigations. A handful of ^{100}Sn ions have recently been observed in two experiments [1,2], and excited states have been identified in neighboring nuclei, e.g., ^{97}Ag [3], ^{98}Ag [4], ^{100}Cd [5], ^{102}In [6], and ^{104}Sn [7]. In this work we report on the observation of excited states in the nucleus $^{99}_{48}$Cd$_{51}$, which has two proton holes and one neutron outside the ^{100}Sn core and is now, together with ^{97}Ag, the closest neighbor to ^{100}Sn with known excited states.

An important property of ^{100}Sn is the degree of rigidity of its spherical equilibrium shape. This is directly related to the excitation energy and transition rates of the lowest 2^+ state. The main wave function component of this state in a microscopic description is an isoscalar mixture of proton and neutron excitations $2d_{5/2}1g_{9/2}^{-1}$ across the $N = Z = 50$ shell closures. This 2_1^+ state will be lowered in energy and its collective strength increased by coupling to the high-lying giant quadrupole vibrations.

The excitation energy and collectivity of the 2_1^+ state in ^{100}Sn are not known from experiment. In the heavy closed-shell nuclei ^{132}Sn and ^{208}Pb, the excitation energies of the 2_1^+ states are 4.04 and 4.09 MeV, respectively, while it is 2.70 MeV in the light $N = Z$ doubly magic ^{56}Ni. The splittings of the relevant single particle states $2p_{3/2}1f_{7/2}$ (^{56}Ni, 6.40 MeV), $2d_{5/2}1g_{9/2}$ (^{100}Sn, ≈6 MeV [8]), $2f_{7/2}1h_{11/2}$ (^{132}Sn, 4.90 MeV), and $2g_{9/2}1i_{13/2}$ (^{208}Pb, 5.07 MeV) are comparable. Since the lowering by the proton-neutron interaction should be particularly effective when the protons and neutrons occupy identical quantum states, it is not unlikely that, as in ^{56}Ni, the 2_1^+ state comes lower in ^{100}Sn than in ^{132}Sn or ^{208}Pb. A $B(E2,\ 2^+ \rightarrow 0^+) = 9(2)$ W.u. was recently measured in ^{56}Ni [9]. As a consequence, the polarization charges for low energy $E2$ transitions in the neighborhood of ^{100}Sn could be enhanced. There is experimental evidence [8] from $B(E2,\ 6_1^+ \rightarrow 4_1^+)$ values in light Sn isotopes down to ^{104}Sn which points to a neutron effective charge of more than $2e$, i.e., about twice as large as the values in the ^{132}Sn and ^{208}Pb regions. However, the analysis of the Sn transition rates is troubled by the difficulty to fix the amount of configuration mixing in the initial and final states. We will show below that the present experiment provides independent and unambiguous information about the $E2$ polarization charge in the ^{100}Sn region.

The experiment was performed at the Tandem Accelerator Laboratory of the Niels Bohr Institute in Denmark using the NORDBALL detector array [10]. A pulsed beam of ^{58}Ni with an energy of 261 MeV was used to bombard a ^{50}Cr target. The energy loss of the ^{58}Ni beam was large enough to produce nuclear reactions in an energy range between the beam energy and the Coulomb

 0031-9007/96/76(6)/888(4)$06.00

barrier. The ^{50}Cr material was enriched to 96.8% and evaporated onto an Au backing, which was thick enough to stop all evaporation residues from reactions on Cr.

The most interesting neutron deficient and unknown residual nuclei are formed in less than 1% of the total population. Thus, besides an efficient γ-ray detector array, a very high reaction channel selectivity is needed for the identification of unknown nuclei. A technique based on the detection of γ rays in coincidence with evaporated charged particles and neutrons was used to select the residual nuclei.

The NORDBALL detector array consisted of 15 BGO shielded Ge detectors with a total photopeak efficiency of about 1%. Light charged particles were detected in 21 ΔE-type Si detectors [11]. The efficiency for detection of protons and α particles was about 60% and 40%, respectively. Neutrons were detected by 11 liquid scintillator detectors [12]. The total neutron detection efficiency was 24%. The detector setup contained also a γ-ray calorimeter composed of 30 BaF_2 crystals. The logical OR signal from the 30 BaF_2 crystals was used as a time reference for all other signals. The BaF_2 detector array supplied information about the total γ-ray multiplicity and the sum energy, which were used to distinguish between different reaction channels as described later. A considerable buildup of ^{12}C took place on the target during the experiment. To be able to distinguish between reactions on ^{12}C and ^{50}Cr we performed an experiment with the same beam but with a ^{12}C target. Further details about both experiments are given in Ref. [13].

The events were sorted into particle gated γ-ray spectra and γ-γ matrices. The nucleus ^{99}Cd was produced by the emission of two α particles and one neutron. However, γ rays belonging to ^{99}Cd contributed to several other $(2\alpha, 1\alpha 1n, \ldots)$ particle gated γ-ray spectra as a result of the limited particle detection efficiencies. A total of 31 different residual nuclei were identified in the main experiment, and the population of ^{99}Cd was only 0.008% of the total yield. Therefore, all the particle gated spectra and matrices were dominated by events that did not belong to ^{99}Cd. In addition, a large number of γ-ray peaks belonging to the main target contaminant ^{52}Cr were also found in the $2\alpha 1n$ gated spectrum. Moreover, there were γ-ray lines present in the spectra originating from reactions on ^{12}C. This was a serious problem in searching for the weak ^{99}Cd channel. A small amount of ^{16}O was present in the targets, and γ rays from transfer reactions leading to residual nuclei in the vicinity of ^{58}Ni and ^{50}Cr were also contaminating the spectra.

To find γ-ray transitions belonging to the weakly populated nucleus ^{99}Cd it was necessary to clean the $2\alpha 1n$ gated spectrum from its contaminating channels as much as possible. This was done by subtracting, with a proper normalization, the $3p2\alpha 1n$, $2p2\alpha 1n$, $1p2\alpha 1n$, and $2p1\alpha 1n$ gated spectra. Each of these spectra was first cleaned in a similar way before the subtraction. The background of the resulting spectrum showed large fluctuations, and it contained several γ-ray lines originating from the ^{12}C (^{58}Ni, $2\alpha 1n)^{61}$Zn reaction. The intensity of the γ-ray lines from the reactions on ^{12}C could, however, be reduced by utilizing the fact that the average γ-ray multiplicity and sum energy are lower in reactions on ^{12}C. By gating on the γ-ray multiplicity and sum energy as obtained from the BaF_2 and neutron detectors, the intensities of the carbon related lines were decreased by a factor of about 10, while the intensities of the remaining lines in the spectrum only decreased by a factor of about 3. These latter γ rays were not present in the experiment on the ^{12}C target, and they were strong candidates for transitions in ^{99}Cd. Further, three lines were found to be delayed, which helped in reducing the background considerably compared to the prompt spectrum. Figure 1(a) shows the cleaned and delayed (10 to 40 ns) $2\alpha 1n$ gated spectrum. It clearly shows three γ-ray lines with energies 226, 607, and 1224 keV. They are assigned to ^{99}Cd as discussed below.

With the assumption that the particle detection efficiency is independent of the reaction channel, the intensities of a specific γ ray in different particle gated spectra depend only on the multiplicities of the particles accompanying the γ-ray emission. Thus, a comparison of the intensity ratio for a specific γ ray in two different particle gated spectra, with the intensity ratios for γ rays from previously known nuclei also observed in the experiment, enables an unambiguous assignment of the final nucleus. Results of such comparisons are shown in Fig. 2. Figure 2(a) shows the intensity ratio of the 1224 keV line as deduced from the spectra gated with one and zero neutrons, respectively. It has a similar value as the γ-ray intensity ratios of two known lines belonging to ^{98}Ag and

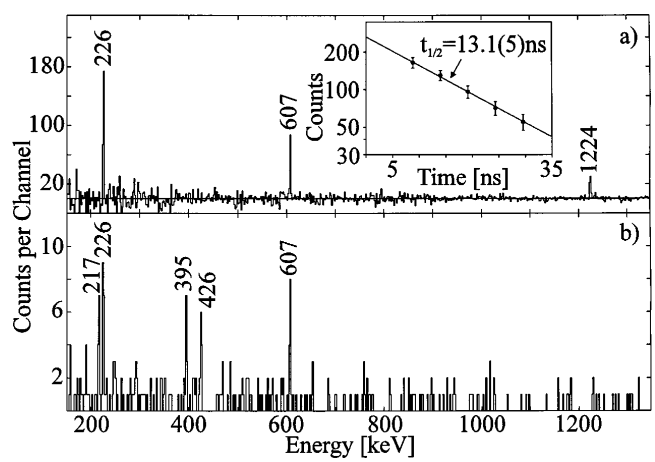

FIG. 1. (a) Cleaned and delayed (10–40 ns) $2\alpha 1n$ gated γ-ray projection and (b) the 1224 keV γ-ray gate obtained from the sum of the $2\alpha 1n$, 2α, $1\alpha 1n$, and 1α particle gated γ-γ matrices. The time distribution of the 1224 keV γ-ray line is shown as an inset in (a).

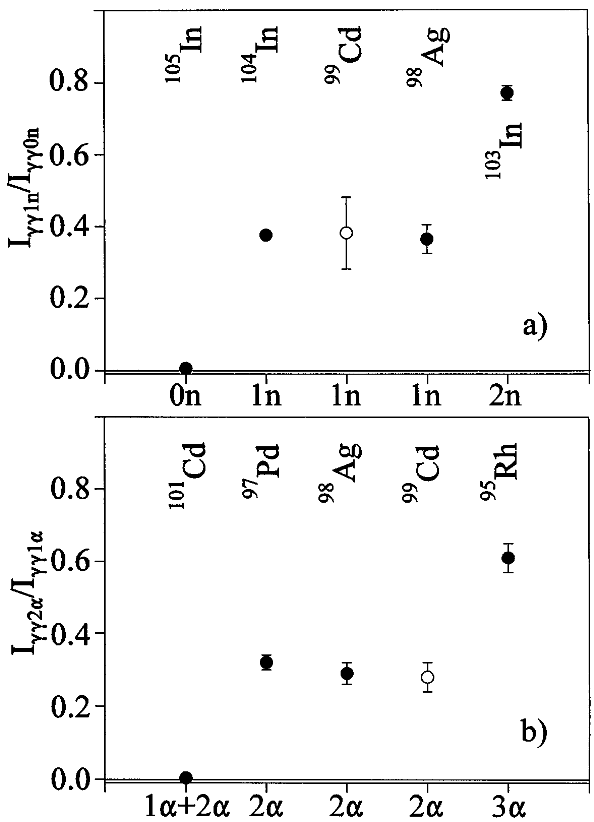

FIG. 2. Intensity ratios for different (a) neutron and (b) α-particle multiplicities.

^{104}In, which are produced in reaction channels where one neutron is emitted. Thus, the 1224 keV line does not belong to a two neutron or to a zero neutron channel, which was observed in one neutron gated spectra due to imperfect n-γ separation. Figure 2(b) shows again the intensity ratio of the 1224 keV line, but in this case extracted from the spectra gated by one and two α particles, which suggests that the 1224 keV line belongs to a 2α channel. Figure 2(b) also shows that this line is not due to an unknown transition in ^{101}Cd, populated in the ^{52}Cr(^{58}Ni, $2\alpha 1n$)^{101}Cd reaction. Known lines in ^{101}Cd behave predominantly as originating from the ^{50}Cr(^{58}Ni, $2p1\alpha 1n$)^{101}Cd reaction as seen from the low ratio in Fig. 2(b). The same conclusions could be drawn for the 226 and 607 keV lines. Further, none of the lines in Fig. 1(a) is in coincidence with protons.

Figure 1(b) shows a spectrum gated by the 1224 keV γ ray. It was obtained from the sum of the $2\alpha 1n$, 2α, $1\alpha 1n$, and 1α gated γ-γ matrices. The matrices contained prompt and delayed γ rays. The γ-ray peaks at 217, 226, 395, 426, and 607 keV are the only peaks in this spectrum that are more than 3σ above the background. The γ-ray gates put in the $2\alpha 1n$ gated matrix and in the summed matrix clearly show that all observed transitions are in mutual coincidence with each other except for the 395 keV transition. For this transition the coincidence relations could not be firmly established due to low statistics in the individual gates. We conclude that the γ rays of Fig. 1 all belong to ^{99}Cd.

The energies, relative intensities, and angular distribution intensity ratios of the six transitions assigned to ^{99}Cd are summarized in Table I. The relative intensities were obtained from the $2\alpha 1n$ gated projection. Due to a high background in that spectrum, the relative intensities contain large statistical errors. The γ-ray angular distribution intensity ratios were obtained from the γ-ray intensities measured in the Ge detectors at 143° with respect to the beam axis divided by the intensity measured in the Ge detectors at 79° and 101°.

Based on relative intensities, angular distribution intensity ratios, coincidence relations, and partly on the systematics of odd A isotones with $N = 51$, we propose the level scheme of ^{99}Cd shown in Fig. 3. The ground state spin and parity of ^{99}Cd are not known, and, therefore, all spins and parities in the experimental level scheme are tentative. However, our shell model calculations suggest $I^\pi = 5/2^+$. This is also suggested from the systematics of the odd A isotones with $N = 51$. It is quite clear (see Fig. 1) that there is a cascade of three delayed γ rays connecting the ground state with the isomeric state at an excitation energy of 2057 keV. All three transitions are consistent with stretched quadrupoles, and we tentatively assign spin and parity of $17/2^+$ to the 2057 keV state. This is similar to the situation in the isotone ^{97}Pd [14] and the ordering of the transitions below the isomer was done according to the systematics. The 217 keV transition is most probably a stretched dipole transition, and the state at 2274 keV is assigned $I^\pi = (19/2^+)$.

The half-life of the state at 2057 keV was determined by putting gates on the delayed part of the γ-ray time spectrum and measuring the intensity of the 1224 keV line in the projected γ-ray energy spectrum. The width of the time window was 5.2 ns, and the result is shown as an inset in Fig. 1. The fit to the experimental intensities is the solid line in the figure, and it corresponds to a half-life of 13.1(5) ns.

Shell model calculations were performed using the RITSSCHIL code [15]. They reproduce the experimental level scheme well, as shown by the comparison in Fig. 3.

TABLE I. Energies, γ-ray intensities, and angular distribution intensity ratios $I(143°)/[I(79°) + I(101°)]$ for γ rays belonging to ^{99}Cd.

Energy (keV)	Relative intensity	Angular distribution intensity ratio
216.7 (3)	7 (8)	0.8 (2)
226.0 (3)	100 (16)	1.7 (4)
395.0 (3)	63 (8)	
426.1 (5)	60 (40)	
606.8 (3)	96 (11)	1.4 (4)
1224.2 (4)	77 (10)	1.3 (3)

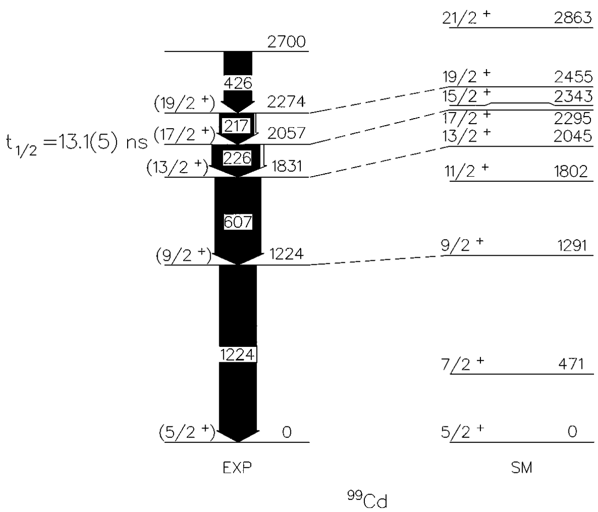

FIG. 3. Experimental and calculated level schemes of ^{99}Cd. The white parts of the arrows show the calculated contribution from internal conversion.

Details about the calculations are given in Ref. [8]. The theoretical interpretation is relatively simple since the nucleus has only two proton holes and one neutron particle relative to the ^{100}Sn core. The calculated lowest lying $5/2^+$, $9/2^+$, $13/2^+$, $17/2^+$, and $19/2^+$ states, which are attributed to five out of six experimental levels in Fig. 3, are all dominated by the $\pi g_{9/2}^{-2} \nu d_{5/2}$ configuration. On the other hand, the calculated lowest $7/2^+$, $11/2^+$, and $15/2^+$ states with no experimental counterparts contain large wave function components with the neutron occupying the $g_{7/2}$ shell. The low relative intensity of the 1224 keV ground state transition (see Table I) may possibly indicate that there is a weak decay branch to the $\nu g_{7/2}$ one quasiparticle state.

The most interesting piece of information of this work derives from the measured half-life of the $17/2^+$ level, which gives $B(E2,\ 17/2^+ \rightarrow 13/2^+) = 68\ e^2\,\mathrm{fm}^4 =$ 2.5 W.u. The main wave function components are $\pi g_{9/2}^{-2} \nu d_{5/2}$ with the proton pair coupled to 6^+ or 8^+ in the initial state and to 4^+ or 6^+ in the final state. The amplitudes of the different angular momentum couplings are relatively insensitive to the detailed assumptions about the effective $\pi\pi$ and $\pi\nu$ interaction matrix elements. The main characteristic that determines the composition of the states is the strong repulsion in the aligned $(\pi g_{9/2}^{-1} \nu d_{5/2})7^+$ particle-hole coupling. This is a common feature of different realistic interactions. With our calculated wave functions the largest contributions to the $E2$ amplitude are given by the protons. The $d_{5/2}$ neutron adds a correction of about 10% to the amplitude, while terms involving $\nu g_{7/2}$ admixture are insignificant. Using the value 26 fm^2 for the diagonal radial integrals of r^2 in the orbitals $\pi g_{9/2}$ and $\nu d_{5/2}$, and the neutron effective charge of $1.0e$, we conclude that the experimental $B(E2)$ value is reproduced by choosing the proton effective charge of $1.6e$. This value is of similar magnitude as the proton effective charge in the ^{132}Sn region [16] and the ^{208}Pb region [17]. Our analysis therefore indicates that the quadrupole polarization of the ^{100}Sn core by protons is not much stronger than is the case for the other heavy doubly magic cores. The full shell model calculation supports this analysis yielding $B(E2) = 87.3\ e^2\,\mathrm{fm}^4$, using effective charges from the ^{90}Zr region $e_{\mathrm{eff}}(\pi) = 1.72e$ and $e_{\mathrm{eff}}(\nu) = 1.44e$ [8]. A natural check of this conclusion in an even simpler case would be provided by a measurement of the half-life and decay energy of the predicted 8^+ isomer in ^{98}Cd.

In conclusion, we have, for the first time, identified excited states in the nucleus ^{99}Cd. The level scheme is well reproduced by a shell model calculation. The analysis of the measured half-life of a $17/2^+$ level gives the proton effective charge of $1.6e$, which indicates that ^{100}Sn has similar stability with respect to quadrupole shape changes as other heavy doubly magic nuclei.

This work was partially supported by the Danish, Finnish, and Swedish Natural Science Research Councils, by the Hungarian Fund for Scientific Research (OTKA Contract No. T7481), and by the Polish Scientific Research Committee (Grants No. KBN2-P03B-02308 and No. KBN2-P03B-04709). The cooperation of the staff at the Tandem Accelerator Laboratory of the Niels Bohr Institute is appreciated. Software written by D. C. Radford was used.

[1] R. Schneider *et al.*, Z. Phys. A **348**, 241 (1994).
[2] M. Lewitowicz *et al.*, Phys. Lett. B **332**, 20 (1994).
[3] D. Alber *et al.*, Z. Phys. A **335**, 265 (1990).
[4] R. Schubart *et al.*, Z. Phys. A **352**, 373 (1995).
[5] M. Gorska *et al.*, Z. Phys. A **350**, 181 (1994).
[6] D. Seweryniak *et al.*, Nucl. Phys. **A589**, 175 (1995).
[7] R. Schubart *et al.*, Z. Phys. A **340**, 109 (1991).
[8] H. Grawe *et al.*, Phys. Scr. **T56**, 71 (1995).
[9] G. Kraus *et al.*, Phys. Rev. Lett. **73**, 1773 (1994).
[10] G. Sletten, *Proceedings of the International Seminar on The Frontier of Nuclear Spectroscopy, Kyoto, 1992* (World Scientific, Singapore, 1993), p. 129.
[11] T. Kuroyanagi *et al.*, Nucl. Instrum. Methods Phys. Res., Sect. A **316**, 289 (1992).
[12] S. E. Arnell *et al.*, Nucl. Instrum. Phys. Res., Sect. A **300**, 303 (1991).
[13] M. Lipoglavšek *et al.*, Proceedings of the International Conference on Exotic Nuclei and Atomic Masses, Arles, 1995 (to be published).
[14] W. F. Piel *et al.*, Phys. Rev. C **41**, 1223 (1990).
[15] D. Zwarts, Comput. Phys. Commun. **38**, 365 (1985).
[16] J. Blomqvist *et al.*, Phys. Scr. **9**, 321 (1974).
[17] G. Astner *et al.*, Nucl. Phys. **A182**, 219 (1972).